VISTA Hemisphere Survey Data Release
Imaging and Catalogue Data Release 5 (DR5)

Data Collection: VHS, VHS_DR5_CATALOGUES
Release Number: 5
Data Provider: Estelle Pons, Richard McMahon, Manda Banerji, Carlos Gonzalez-Fernandez and the VHS collaboration
Date: DD.MM.2020

Abstract:

The VISTA Hemisphere Survey (VHS; ESO Programme ID: 79.A-2010) is a wide field near infrared survey, which when combined with other VISTA public surveys will result in coverage of the whole southern celestial hemisphere (Declination $< 0°$; $\sim 20,000 \deg^2$) to a depth 30 times fainter than 2MASS/DENIS in at least two wavebands (J and K_s), with a minimum exposure time of 60 seconds per waveband and a median 5σ point source depth of AB = 20.8 and 20.0 in J and K_s wavebands respectively. In the South Galactic Cap, around 4500 $\deg^2$ is being imaged deeper with an exposure time per coadded image of 120–240 seconds in J, 120 seconds in K_s and partial coverage in H band with an exposure time of 120 seconds, producing median 5σ point limits of AB = 21.4, 20.7 and 20.3 in J, H and K_s respectively. In this 4500 $\deg^2$ region of sky deep multi-band optical (grizY) imaging data is being provided by the Dark Energy Survey (DES). The remainder of the high galactic latitude ($|b| > 30°$) sky is being imaged in Y, J, K_s for 60–120 sec per band with median 5σ point source limits of AB = 21.1, 20.8 and 20.0 and partial coverage in H with a median 5σ point source limit of 20.3. This region is being imaged in the optical wavebands (ugriz) by the the VST ATLAS survey. The median 5σ point source depths for the total survey area coadd images in this data release is AB=21.1, 20.8, 20.5, 20.0 in Y, J, H and K_s wavebands respectively.

This data release (DR5) contains 11370 tile level multi-band source catalogues based on 3226 Y band, 11332 J band, 1961 H band and 11326 K_s band tiles derived from VHS observations taken over a 8 year period between the start of the survey (UT date of 2009 November 04) during ESO Observing Period 84 and the end of ESO Observing Period 98 (UT date of 2017 March 31). There are a total of 1,374,207,485 sources including sources detected in a single waveband. The sky coverage is 4825 $\deg^2$, 16689 $\deg^2$, 2901 $\deg^2$, 16684 $\deg^2$ in Y, J, H and K_s respectively. The coverage in at least one waveband covering is 16,730 $\deg^2$ of sky.

In addition to the multi-band source catalogues described above, this data release contains the first public ESO release of multi-extension FITs (MEF) format pawprint image files, FITS format tile images, weight map images and single band tile source lists for observations obtained during ESO Observing periods 96 to 98 (UT date range 2015 October 1 to 2017 March 31 inclusive). The release also contains image products and single band source lists for Period 95 (date range 2015 April to 2015 Sep 30) which were previously released in data release DR4, and were reprocessed with a more recent version of the CASU pipeline software (version 1.5).

This data release contains data which has primarily been processed with version 1.5 of the CASU pipeline. Changes since version 1.3 of the CASU pipeline include an updated photometric calibration and updates to the Galactic extinction coefficients used in generating the photometric zero-points (see González-Fernández et al. (2018) for more details). In most fields the zero-point change is at the level of 1% to 2%.

Contents

1 Overview of Observations

The VISTA telescope (Sutherland et al., 2015) camera VIRCAM (Dalton et al., 2006) consists of a sparse filled mosaic of 16 2k × 2k Raytheon Mercury Cadmium Telluride (MCT) detectors with $20\mu m$ square pixels with a mean celestial scale of 0.339" per pixel. Each single observations is called a pawprint. A series of spatially contiguous pawprint observations produced an infilled contiguous image called a tile and consists of combining a sequence of six offset pawprints that fill the gaps on the sky between the individual detectors. All VHS tiles are observed with a rotator-sky angle of 180°; thus each tile covers a rectangle approximately 1.5° in Right Ascension (RA) by 1.0° in Declination. The tiling pattern used is Tile6zz as described in the VISTA Users Guide (https://www.eso.org/sci/facilities/paranal/instruments/vircam/doc/VIS-MAN-ESO-06000-0002_v101.pdf; see also the SADT manual at https://www.eso.org/sci/observing/phase2/VIRCAM/SADT_cookbook_v2.1.pdf). Each pawprint imaging sequence consists of 2 jitters with a jitter size of 20 arc secs. Normally a Jitter pattern Jitter2d or Jitter2da was used apart from during the 'Dry Run' period that preceeded the

start of the nominal survey when some other patterns were used to verify the observing strategy.

The VHS survey is divided into 3 components for survey planning and management and purposes, based on their common OB structures. These components in alphabetic order are described below with their nominal coverage as defined in the VHS survey management plan (McMahon et al, 2007):

- VHS-ATLAS ($\sim 5000 \deg^2$); consists of two regions of sky, one in the north galactic cap(NGC; $\sim 2500 \deg^2$) and the second in the south galactic cap (SGC; $\sim 2500 \deg^2$) to be observed in YJHK$_s$ for 60 seconds per waveband.

- VHS-DES ($\sim 4500 \deg^2$); a contiguous region of sky in the SGC to be observed in JHK$_s$ for 120 secsonds per waveband.

- VHS-GPS ($\sim 8200 \deg^2$); A region of lower galactic latitude which we define as the VHS Galactic Plane Survey (GPS) with $5° < |b| < 30°$ ($\sim$8200 deg^2); excluding the VVV and VMC regions; to be observed in J and K$_s$ for 60 seconds per waveband.

The spatial coverage of VHS can be divided into three contiguous regions of the celestial sphere:

1. VHS-NGC (North Galactic Cap): $b > 30°$; $\delta < 0°$ ($\sim 2500 \deg^2$); excluding the VIKING NGP region. This is the NGC part of VHS-ATLAS. The baseline exposures of 60 seconds per band in YJHK$_s$.

2. VHS-SGC (South Galactic Cap): $b < -30°$; $\delta < 1.0°$ ($\sim$7000 deg^2); excluding the VIKING SGC region and VMC region. JHK$_s$ for 120 secs over VHS-DES region on the assumption that Dark Energy Survey (DES) project will project provide matching Y and Z waveband observations. This is defined as the VHS-DES region and is 4500^2 in sky area. The DES footprint is defined below. YJHK$_s$ for 60secs over the remainder of the SGC starting with the region to be covered with the VST ATLAS survey (note that some the VST-ATLAS survey lies within the VHS-DES footprint). This region is the SGC part of the VHS-ATLAS.

3. VHS-GPS (Galactic Plane Survey): as described above.

The proposed footprint (circa 2007) of the Dark Energy Survey(DES) consisted of three connected regions in the SGC.

- 20hrs $< \alpha <$ 7hrs; $-65° < \delta < -30°$ and 19hrs $< \alpha <$ 20hrs; $-65° < \delta < -45°$; 4000 deg^2; South Pole Telescope(SPT) survey region

- 1.3hrs $< \alpha <$ 3.4hrs; $-65° < \delta < -30°$; 800 deg^2

- 20.6hrs $< \alpha <$ 3.4hrs; $-1° < \delta < 1°$; 200 deg^2; SDSS Stripe82

Each tile is observed in multiple wavebands in the same observing blocks (OBs) with an on-sky time execution time per OB of 360 seconds to 1080 seconds. The area of VHS-DES footprint is assumed to be 4500 deg^2 out of the full DES footprint of 5000 deg^2 since part of VIKING survey footprint overlaps with the DES footprint as shown in Figure 1.

In Period 89, following consultation with the PSP we changed the observing strategy in order to increase the exposure time in the bluest wavebands in the DES and ATLAS components and removed the H band observations from these OBs. This reduced the execution time per OB for these OBs by 280 seconds i.e 15%. The actual on sky exposure time for future OBs is now:

1. VHS-GPS: J (60 seconds) ; K_s (60 seconds)

2. VHS-ATLAS: Y(120 seconds); J (60seconds) , K_s (60 seconds)
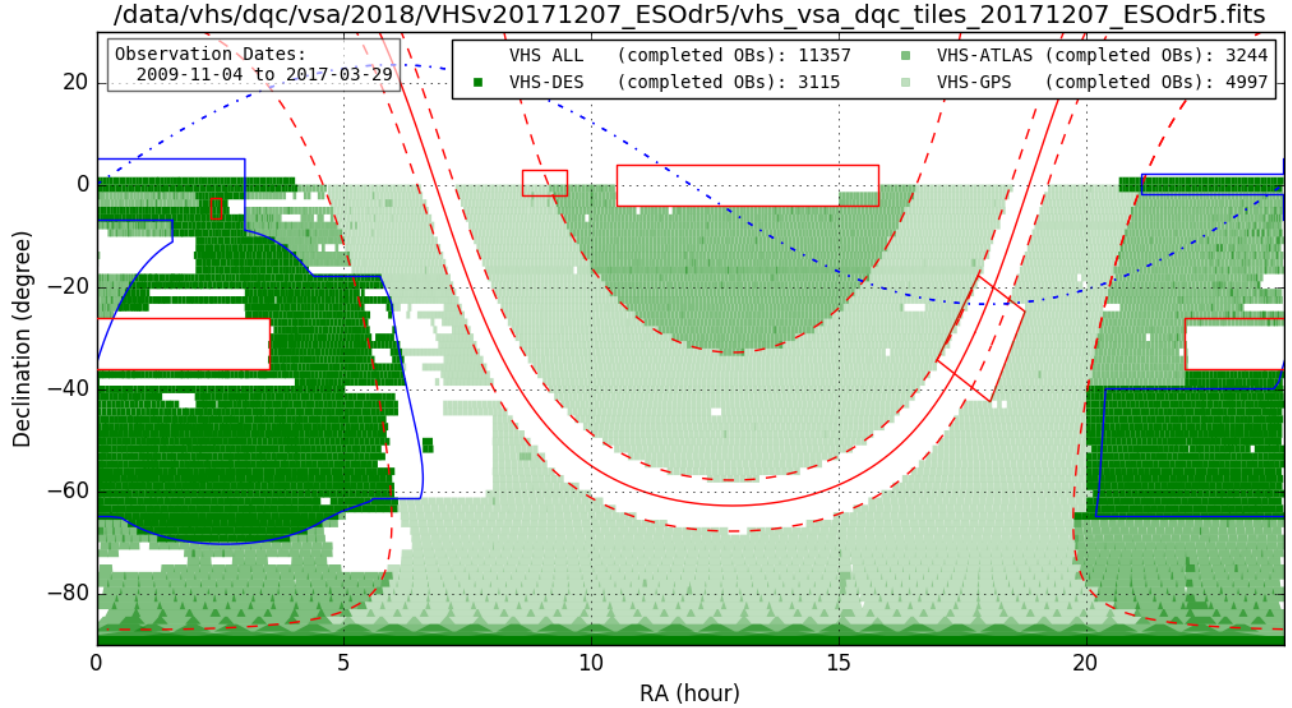
3. VHS-DES: J (240 seconds), K_s (120 seconds)

Figure 1: Sky coverage for this data release showing the total area covered (around 16,730 deg^2) in at least one filter as green rectangles. The blue polygon shows the DES footprint. The thick red dashed and continuous lines show galactic latitude of b=-30°, -5°, +5°, +30°. The red rectangles show the nominal VISTA VIKING and VISTA VVV survey footprints which are excluded from the VHS observations. The blue dash dotted line show the ecliptic. The legend table lists completed OB statistics for the full VHS area and for the individual survey components (i.e. DES, ATLAS and GPS).

2 Release Content

The sky coverage of the observations that make up this data release (DR5) is summarised in Figure 1 that plots the RA and Dec distribution of all VHS tiles observed in at least one waveband. Figures 2–5 show the coverage for each the four waveband observed in VHS; Y, J, H and K_s.

This data release contains data which has primarily been processed with version 1.5 of the CASU pipeline. Changes since version 1.3 of the CASU pipeline include an updated photometric calibration and updates to the Galactic extinction coefficients used in generating the photometric zero-points, together with a fix for a low-level systematic photometric variation across tile catalogues (see González-Fernández et al. (2018) for more details). The photometric recalibration, which mainly involves changes
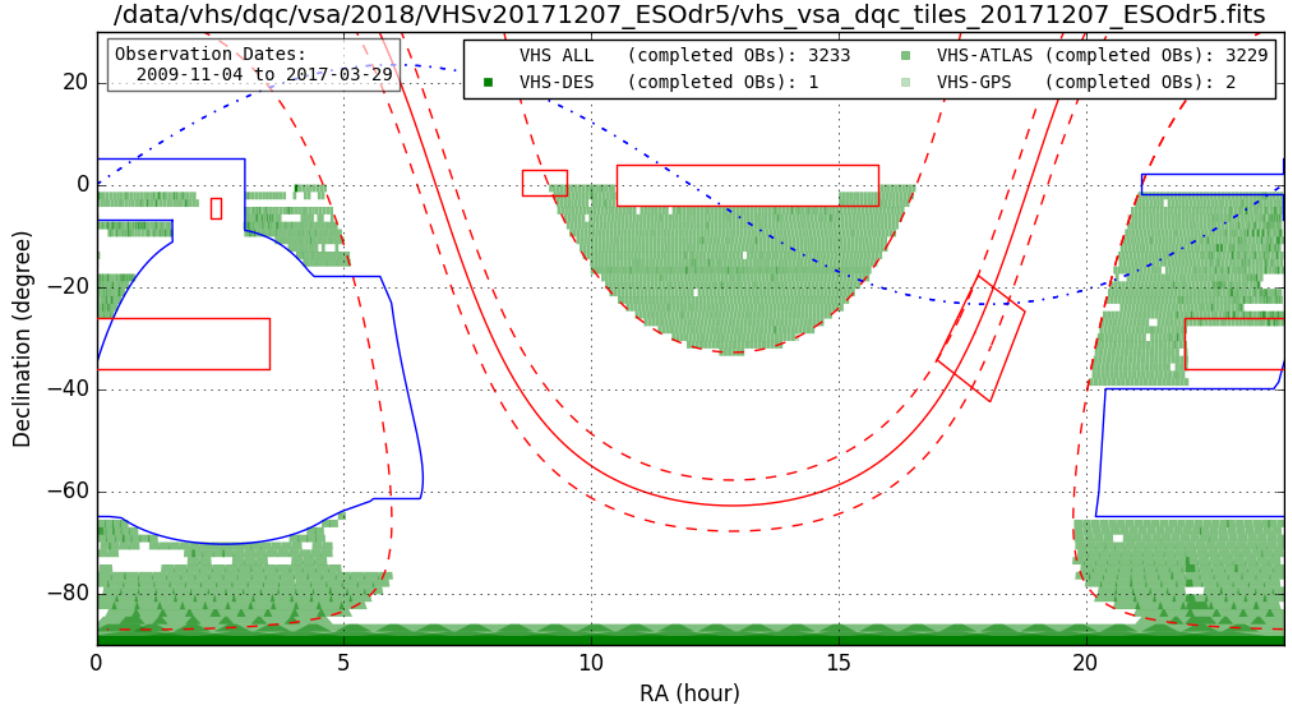
Figure 2: Sky coverage of the fields in this release in the Y waveband (4,825 deg^2). There are 2 OBs that are identified as GPS and 1 OB identified as a DES OB in error. See caption for Figure 1 for explanation of lines and colours.

to tile products, is being back-propagated to data taken before 2017 January 1 and these reprocessed catalogue will be published in a future data release. In most fields the zero-point change is at the level of 1% to 2%.

This data release (DR5) includes all tile level multi-band source catalogues from VHS observations taken between the start of the survey (UT date of 2009 November 04) during ESO Observing Period 84 and the end of ESO Observing Period 98 (UT date of 2017 March 31). It contains 11370 tile level multi-band catalogues based on 3226 Y band tiles, 11332 J band tiles, 1961 H band tiles and 11326 K$_s$ tiles with coverage of 4825 deg^2, 16689 deg^2, 2901 deg^2, 16684 deg^2 in Y, J, H and K$_s$ respectively. The coverage in at least one waveband is 16,730 deg^2 of sky. There are a total of 1,374,207,485 sources including sources detected in a single waveband.

Tile level multi-band catalogues in previous VHS releases (e.g. DR4) for observations obtained up to the end of ESO Observing Period 95 (UT date of 2015 Sep 30) are superseded by this release. Multi-band source catalogues for tiles observed before the 1st January 2017 are based on products processed with CASU pipeline version 1.3 (see Section 3.1). Multi-band source catalogues for tiles observed after 1st January 2017 used CASU pipeline version 1.5 (see Section 3.2).

This data release also includes:

1. The first public ESO release of multi-extension FITs (MEF) format pawprint image files, FITS format tile images, weight map images and single band tile source lists for ESO Observing periods 96 to 98 (UT date range 2015 October 1 to 2017 March 31 inclusive). These data products have
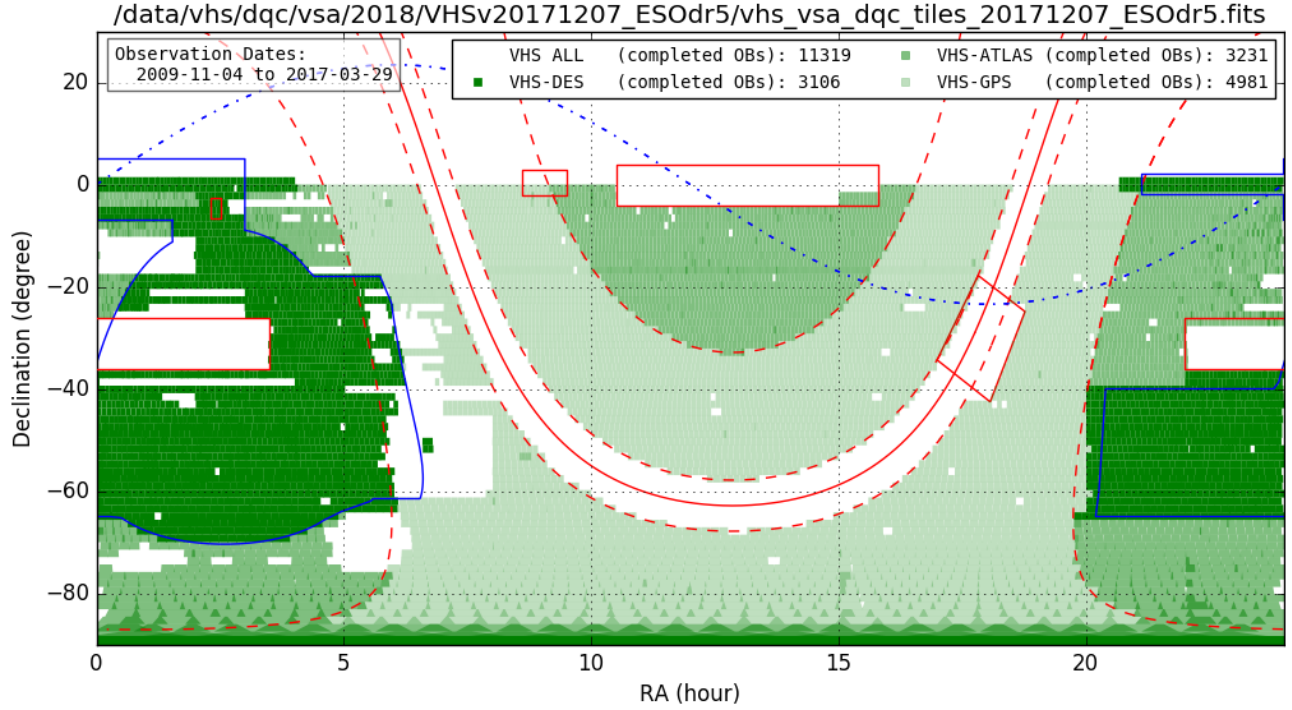
Figure 3: Sky coverage of the fields in this release in the J waveband (16,689 deg^2). See caption for Figure 1 for explanation of lines and colours.

all been processed by CASU pipeline version 1.5.

2. Pawprint and tile image products, and single band tile source lists for Period 95 (date range 2015 April to 2015 Sep 30) which were previously released in data release DR4, and were reprocessed with version 1.5 of the CASU software. A future date release will contain images and single source lists for observations before 2015 April (i.e. Periods 84 to 94) processed by CASU pipeline version 1.5.

Pawprint images, single band tile images and single band source list products prior to ESO Observing Period 95 are unchanged (i.e Periods 84 to 94). The FITS files have a keyword 'PROCSOFT' that specifies the version of the CASU software used. e.g. PROCSOFT = 'CASU_VIRCAM_Version_1.5' which can be used to determine the version of the CASU pipeline software used to produce a data product.

3   Release Notes

These release should be read in conjunction with the documentation provided at:

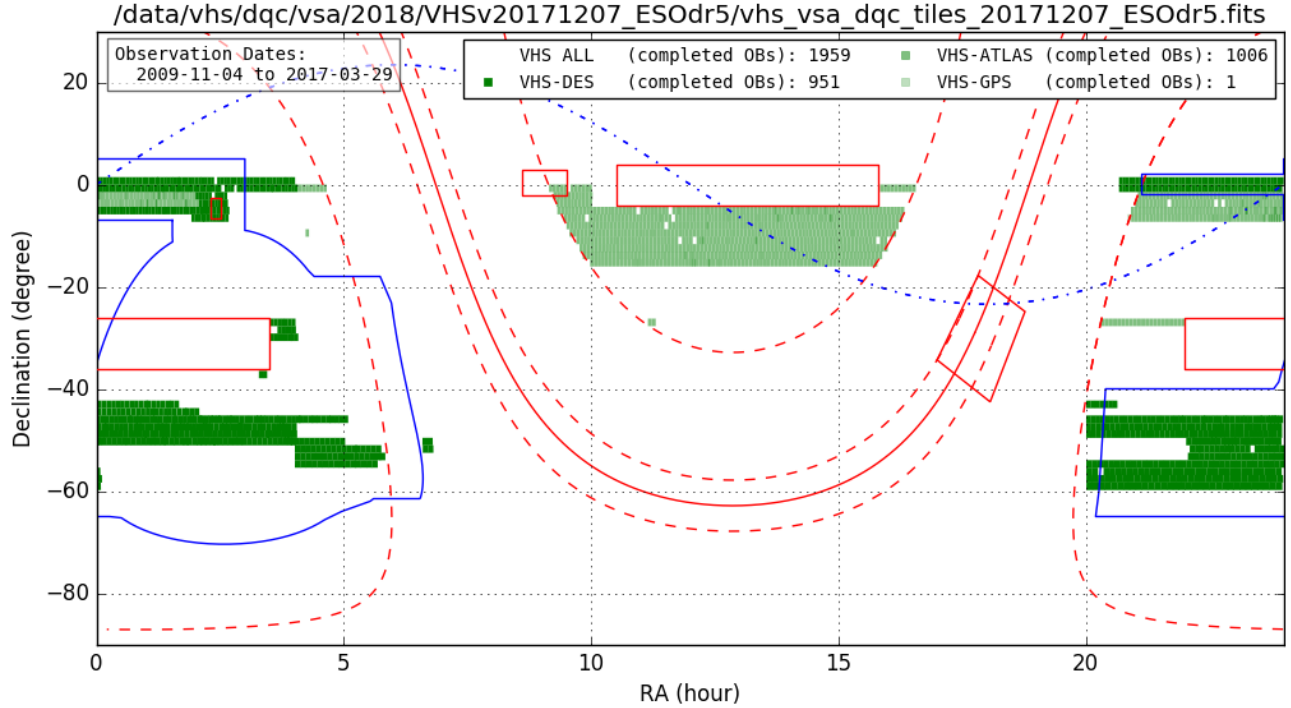- CASU: http://casu.ast.cam.ac.uk/surveys-projects/vista/technical

- WFAU: http://horus.roe.ac.uk/vsa/

/data/vhs/dqc/vsa/2018/VHSv20171207_ESOdr5/vhs_vsa_dqc_tiles_20171207_ESOdr5.fits

Figure 4: Sky coverage of the fields in this release in the H waveband (2,901 deg^2). There is currently 1 OB that is identified as a GPS OB in error. See caption for Figure 1 for explanation of lines and colours.

The CASU pipeline version 1.3 (27/03/2013) and 1.5 (observations made after 01/01/2017) are used for the data products in this release. Note that version 1.4 was used for CASU internal testing and no pipeline version 1.4 data has been released externally.

3.1 CASU pipeline version 1.3 (2013/03/27)

The main catalogue changes for version 1.3 are:

1. A bug involving how the aperture 2 correction was calculated is now fixed and tile catalogues have now been regrouted to include this.

2. Prior to regrouting all the stacked pawprint photometric zero-points were recomputed using the latest version of the photometry software.

3. Post regrouting all the tile photometric zero-points have also been updated.

4. ESO grades have been updated and they should now agree with those supplied by ESO to the PIs directly. This affects the keywords ESOGRADE and OBSTATUS for all data products. See the ESO Grades page for more information on their values.

5. All tile catalogues have been re-grouted taking into account both detector level magnitude zero points variations (tiles before 20101101 did not have those applied) and atmospheric seeing variations.
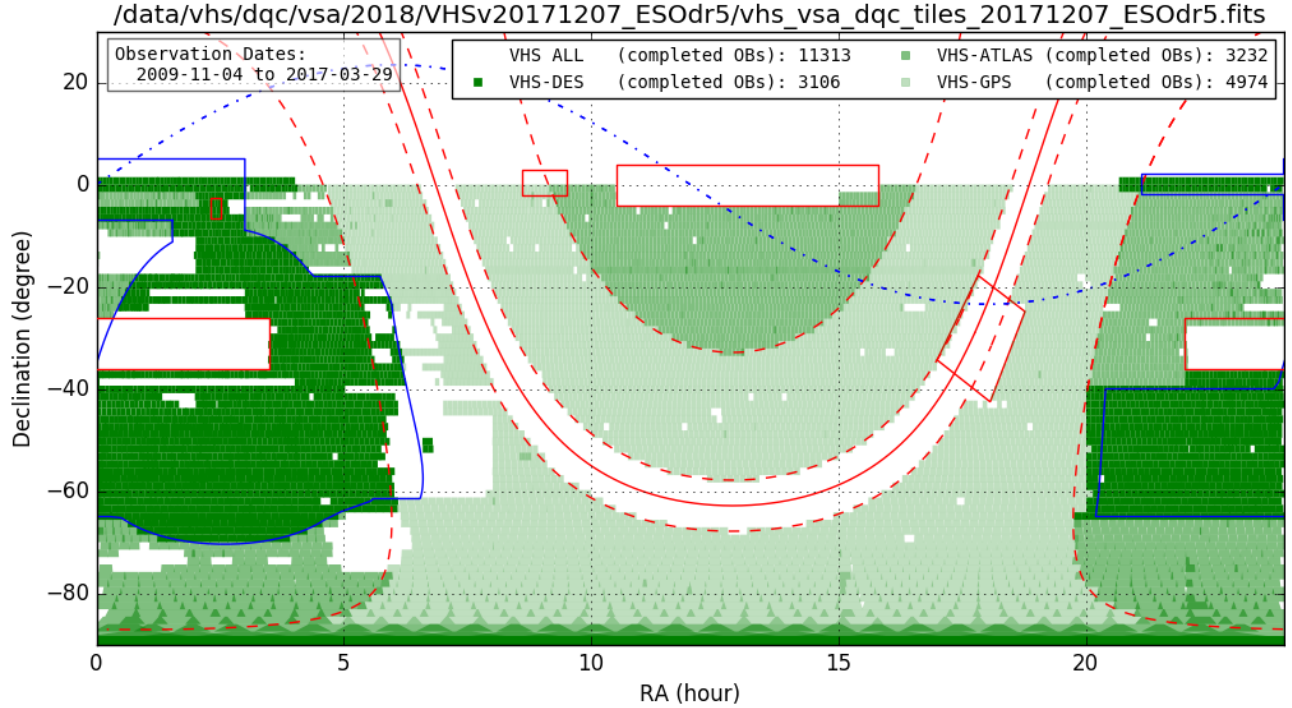
Figure 5: Sky coverage of the fields in this release in the K_s waveband (16,684 deg^2). See caption for Figure 1 for explanation of lines and colours.

6. Note that WCS coefficients for PV2$_3$ and PV2$_5$ were changed from 42.0, - 10000.0 pre-20101130 to 44.0, -10300.0 post-20101201. The pre-20101130 astrometry was not updated.

7. The internal ZPN-TAN definition bug that affected tile products was fixed August 2012. All products post-2012801 use the corrected ZPN-TAN transformation. Earlier tile products remain affected at the ∼100mas level by this bug. All pawprint products are unaffected.

3.2   CASU pipeline version 1.5 (2017/01/01)

All observation taken after the start 2017 (i.e. 2017 Jan 01 onwards) have been processed with CASU pipeline version 1.5 (Note that version 1.4 was used for internal testing and no official version 1.4 data has been released externally.) Changes since version 1.3 include an updated photometric calibration and updates to the Galactic extinction coefficients used in generating the photometric zero-points, together with a fix for a low-level systematic photometric variation across tile catalogues (see González-Fernández et al. (2018) for more details). The photometric recalibration, which mainly involves changes to tile products, is being gradually back-propagated from 20161231 and will be released as it is checked out. Note that all processed pawprint images and catalogues are unchanged apart from updated magnitude zero-points. In most fields the zero-point change is at the level of 1% to 2%.

The main changes for CASU pipeline version 1.5 are:

1. Updated tile images taking account the changes in stacked pawprint zero-points.

2. Regrouted tile catalogues using photometric zero-points computed using version 1.5 of the photometry software.

3. A fix to the systematic photometry issue which affected all tile catalogues prior to 01/01/2017.

An astrometric issue at the level of 50milli arc seconds for mosaiced tile images was identified by the VHS team and presented at the ESO Surveys conference in Oct 2012. This has been fixed for tiles image data processed post-20120101. See sub-section for further information.

4 Data Reduction and Calibration

The data in this data release have been reduced and calibrated using with the VISTA Data Flow System as described in Irwin et al. (2004), Lewis et al. (2010) and Cross et al. (2012).

4.1 Data processing steps

In brief, the data processing steps are as follows:

4.1.1 Reset correction

This occurs in the data acquisition system, i.e. a VISTA data frame is a difference of two non-destructive detector readouts separated by DIT seconds. Then, NDIT of these frames are co-added within the data acquisition system, before saving to hard disk.

4.1.2 Dark subtraction

Dark subtraction uses exposures with an opaque "dark" filter inserted, with expsoure times matching the DIT values of the relevant science exposure.

4.1.3 Linearity correction

The VIRCAM detectors show non-linearity, typically a few percent at 10,000 ADUs (Analoge to Digital Units). A correction polynomial (one per detector) is derived from a fit to observations of the dome screen with varying exposure times and applied to the counts.

4.1.4 De-striping

This step removes a low-level horizontal striping intrinsic to the VIRCAM detector readout electronics, which is correlated across blocks of 4 detectors.

4.1.5 Flat-field correction

Each science observation image is divided by a flat-field frame, derived from a set of twilight sky flats in the matching relevant filter band.

4.1.6 Bad pixel rejection

Pixels showing substantial deviance from the linearity frames are masked as bad, and assigned zero weight in subsequent combinations.

4.1.7 Sky background correction

Background sky images for each wavebands are generated from all images taken for a single tile to remove large-scale background variation.

4.1.8 Jitter stacking

The set of individual jittered frames for one pawprint-filter combination are combined into a pawprint image, with bad-pixel rejection. These individual pawprint images are available in the data release.

4.1.9 Astrometric and Photometric calibration

This is based on matching with 2MASS (Skrutskie et al., 2006) catalogue stars (see Sections 4.2 and 4.3).

4.1.10 Tiling

The six individual pawprint images for one filter are combined into a full tile image.

4.1.11 Grouting

When combining images into a full tile, there are non-negligible PSF variations across the tile, due mainly to seeing variations between the six individual pawprints, and also slight variation in image quality with off-axis distance. Different pairs of pawprints contribute to different regions in the tile, thus the aperture correction varies with position. A specific correction for this (aka "grouting") is applied to the photometry in the catalogues. The effect of the grouting correction is shown in Figure 6 in González-Fernández et al. (2018).

4.2 Astrometric Calibration

Astrometric calibration is based on stars in the 2MASS (Skrutskie et al., 2006) catalogue; there are typically around 50 unsaturated 2MASS stars per VIRCAM pawprint detector and around 2000 per tile. The astrometric transformations from detector or tile pixel cartesian coordinates to RA, Dec are derived from these astrometric reference stars. The typical rms is 0.15 arcsec per star per coordinate, which is dominated by photon noise in the 2MASS data. 2MASS observations were obtained between 1997 June and 2001 Feb and therefore have a mean epoch of 2000. The reference frame is the International Celestial Reference System (ICRS) via the Hipparcos Tycho-2 Reference Catalog.

Figure 6 shows the distribution of the World Cooordinate System (WCS) rms astrometric errors derived from 2MASS catalogue stars. The J and K_s bands have a tail to smaller rms values compared

to Y and H, since there are J and K_s observations in regions of higher stellar density at lower galactic latitude ($|b| < 30°$) and shows the expected correlation between the number of stars and the rms residuals due to better determination of the WCS transformation. There is plateau in the distribution in the J and K_s bands at a high stellar number density or around 4000 stars per tile. The origin is under investigation and could be a feature of sigma clipping of outliers. The horizontal feature at around 1200 stars only appears for data from P84 and P85. The origin of this effect is not currently known and reflect either a real effect in the released data or could be an issue with the DQC metadata database.

Figure 7 shows a comparison between VHS positions and the VLBI radio reference frame (Petrov (2019), http://astrogeo.org/vlbi/solutions/rfc_2019a). The results are summarized in Table 1 and compared with the results for 2MASS for the same sample of sources. The error in the systematic offsets are derived from the robust σ_{MAD} estimator of the dispersion:

$$\sigma_{offset} = \sigma_{MAD}/\sqrt{N-1}$$

Table 1: Comparison with ICRS VLBI radio reference frame (2019a)

Survey	Number of sources	Systematic offset		Statistical uncertainty	
		RA	Dec	RA	Dec
VHS-DR5	5034	0.005 ± 0.002	0.054 ± 0.001	0.120	0.095
2MASS	4913	-0.002 ± 0.002	0.007 ± 0.002	0.130	0.133

4.3 Photometric Calibration

Photometric calibration is derived from 2MASS stars as described in González-Fernández et al. (2018). The set of colour equations are used to predict VISTA native magnitudes from the observed 2MASS J, H, K_s colours. The colour equations for version 1.3 and for version 1.5 of the CASU VIRCAM pipline are given below.

4.3.1 CASU pipeline version 1.3 colour equations

The version 1.3 colour equations are as follows:

$$Y_V = J_{2M} + 0.610\,(J_{2M} - H_{2M})$$
$$J_V = J_{2M} - 0.077\,(J_{2M} - H_{2M})$$
$$H_V = H_{2M} + 0.032\,(J_{2M} - H_{2M})$$
$$K_{sV} = K_{2M} + 0.01\,(J_{2M} - K_{2M})$$

where in the above, subscript 2M denotes 2MASS and V denotes VHS. The above equations give the predicted VISTA-system Vega magnitudes of 2MASS stars.

4.3.2 CASU pipeline version 1.5 colour equations

The version 1.5 colour equations are as follows.

$$Y_V = J_{2M} + 0.457\,(J_{2M} - K_{2M})$$
$$J_V = J_{2M} - 0.031\,(J_{2M} - K_{2M})$$
$$H_V = H_{2M} + 0.015\,(J_{2M} - K_{2M})$$
$$K_{sV} = K_{2M} - 0.006\,(J_{2M} - K_{2M})$$

In biggest change between version 1.3 and version 1.5 is the use of $(J_{2M} - K_{2M})$ for all wavebands which González-Fernández et al. (2018) report is more stable with respect to galactic latitude as the slope of the colour term is less effected by the relative abundance of late type dwarfs as a function of galactic coordinates.

4.3.3 Conversion from Vega to AB magnitudes

Note we have converted the native VISTA Vega mags to AB ($m_{AB} = m_{Vega} + C_{VegaToAB}$) using the below correction ($C_{VegaToAB}$):

1. For CASU pipeline version 1.3, $C_{VegaToAB} = (0.618, 0.937, 1.384, 1.839)$ for (Y, J, H, K_s) respectively (see http://casu.ast.cam.ac.uk/surveys-projects/vista/technical/filter-set).

2. For CASU pipeline version 1.5, $C_{VegaToAB} = (0.600, 0.916, 1.366, 1.827)$ for (Y, J, H, K_s) respectively (see González-Fernández et al., 2018, Appendix D).

4.4 Star-galaxy classification

A star-galaxy classification parameter (ClassStat) is provided in the list files; this is intended to be approximately Gaussian N(0,1) for stellar objects, and extends to large positive values for galaxies. Also an integer-based classification (Class); see description below. The band-merged catalogue file contains also merged statistics based on a quasi-Bayesian combination of the single-band classifications.

5 Multi-band source catalogue description

The tile level multi-band source catalogues are created from the cross-matching of single band source lists. This cross-matching band merging process is outlined in more detail in the VSA documentation and Cross et al. (2012) but involves the creation of a `vhsSource` table from the individual `vhsDetection` tables. The matching iterates through the catalogues for each band in turn (bluer to redder) and matches can include any combination of filters (one to four from Y, J, H, K_s) depending on how many filters it is detected in.

These single band source list tables are linked via source list reference ID numbers. The matching is done within a default radius of 2.0 arcsec and the selection between multiple potential matches can be made using the `priOrSec` (primary or secondary) flag. The PRIMARY_SOURCE flag has been added to provide an indication which one of the duplicates created in overlap regions between tiles should be used. The user is advised to consult with the VSA documentation and Cross et al. (2012) for more details about these flags and the band merging process.

Table 2 describes a subset of the parameters in the multi-band source catalogue tables as given in the VSA database. A description of all the columns in the multi-band source catalogues delivered in this release with their UCDs is given in Table 4.

We recommend that users should restrict their analysis to objects with `yppErrBits`, `jppErrBits`, `etc`<255 at all times and `yppErrBits`=0 if they require the most reliable subset of the sources. Values of `yppErrBits`=16 indicate that the source was deblended, `yppErrBits`=64 that at least one bad pixel was within the default aperture and `yppErrBits`=128 that the source was low confidence within the default aperture.

Table 2: A summary of the most relevant parameters in the band-merged multi-band source catalogues

`ra, dec:`	RA, Dec in J2000 decimal degrees.
`ra, dec:`	RA, Dec in J2000 decimal degrees.
`l, b:`	Galactic coordinates, decimal degrees.
`yXi, yEta, etc:`	Source offsets from master position in each of the four bands Y, Y, H, K_s; in arcsec East and North respectively.
`priOrSec:`	Integer flag for "primary" or "secondary" source. Objects with priOrSec = 0 are unique to this tile. Objects with priOrSec = frameSetID are "primary" objects on this tile, with a secondary detection on another tile. Objects with priOrSec>0 and priOrSec != framesetID are "secondary" objects with a "primary" detection on a different tile.
`ySeqNum, jSeqNum, etc:`	Sequence number, enabling matching this entry to the corresponding single-band detection.
`ymjPnt, jmhPnt, hmksPnt:`	Respectively colours Y-J, J-H, H-K_s assuming a point source, from the corresponding AperMag3 values.
`ymjExt, jmhExt, hmksExt:`	Respectively colours Y-J, J-H, H-K_s assuming an extended source (using 2 arcsec aperture with no aperture correction).
`yAperMag3, yAperMag4, yAperMag6,` `yAperMagNoAperCorr3, yPetroMag,` `ySerMag, yPsfMag, etc:`	A subset of the various magnitude measures for all the single passbands, beginning with one of y,j,h,ks denoting passband. Here, a subset is given to reduce line length: of the many AperMagN values, only AperMag3,4,6 are given here, and the corresponding versions without aperture correction.
`yClass, yClassStat, etc:`	Respectively integer and real classification flag for each of the single bands.
`mergedClass, mergedClassStat:`	Band-merged integer and real classification, based on a quasi-Bayesian combination of the individual passbands.
`pStar, pGalaxy:`	Probability that the object is stellar/galaxy, respectively.
`pNoise, pSaturated:`	Probability that the object is noise/saturated, respectively.
`yppErrBits, jppErrBits, etc:`	Integer error bits code for each of Y, J, H, K_s bands. Value Zero = no warnings, 1-255 indicates "Warning" level, and any `ppErrBits` value >256 indicates potentially more serious problems.
`PRIMARY_SOURCE`	Integer flag to select between multiple entries in the catalogue. If the value is 1 then this is the 'primary' entry for the source, i.e. priOrSec=0 or priOrSec=frameSetID. If the value is 0 then that entry is a duplicated source, usually a source in an overlap region between fields or tiles.

6 Data quality

6.1 Survey Depth

The 5-sigma point source sensitivity (AB magnitudes) are given in Table 3 for each ESO observing period and each survey component. See Section 4.3 for information on the conversion of the VIRCAM

natural magnitude system which is on the Vega system to the AB magnitude system. The depth versus cumulative area per band for all observations and for each survey component is shown in Figure 8. The median 5σ point source depths for the total survey area in this data release is AB=21.1, 20.8, 20.5, 20.0 in Y, J, H and K_s wavebands respectively.

Table 3: 5-sigma point source sensitivity (AB magnitudes)

Period	ATLAS				DES			GPS		All			
	Y	J	H	K_s	J	H	K_s	J	K_s	Y	J	H	K_s
84	20.92	20.84	20.43	20.00	21.17	20.77	20.43	20.76	19.96	20.91	20.86	20.69	20.05
85	20.77	20.72	20.26	20.08	21.19	20.78	20.46	20.56	19.98	20.77	21.00	20.26	20.07
86	20.67	20.68	20.22	19.95	21.01	20.52	20.31	20.42	19.78	20.67	20.71	20.43	20.00
87	20.79	20.73	20.25	19.93	21.23	20.77	20.39	20.56	19.82	20.79	20.74	20.55	19.96
88	20.91	20.75	20.34	19.99	21.15	20.71	20.36	20.86	20.01	20.91	20.96	20.54	20.15
89	21.38	20.96	20.55	20.10	21.55	-	20.40	20.79	19.85	21.38	20.97	20.55	20.08
90	21.42	20.89	-	20.01	21.47	-	20.33	20.87	19.96	21.42	21.26	-	20.22
91	21.13	20.66	-	19.96	21.53	-	20.35	20.69	19.94	21.13	20.86	-	20.02
92	21.24	20.80	-	19.98	21.37	-	20.21	20.61	19.87	21.24	20.84	-	19.96
93	21.27	20.84	-	20.00	-	-	-	20.74	21.00	21.27	20.78	-	19.98
94	21.20	20.71	-	19.81	21.57	-	20.25	20.70	19.86	21.20	20.82	-	19.93
95	21.18	20.77	-	19.92	21.35	-	20.16	20.60	19.84	21.18	20.66	-	19.86
96	21.12	20.66	-	19.84	21.40	-	20.21	20.60	19.72	21.12	20.67	-	19.78
97	21.09	20.68	-	19.84	21.61	-	20.30	20.55	19.77	21.09	20.66	-	19.82
98	21.07	20.71	-	19.78	21.50	-	20.26	20.52	19.65	21.07	20.90	-	19.90
All	21.13	20.80	20.31	19.98	21.41	20.73	20.33	20.65	19.87	21.13	20.82	20.52	19.99

Note: The method to compute the magnitude limits uses a `MANGLE` mask (Hamilton & Tegmark, 2004, Swanson et al., 2008) to take account the overlap between tiles.

6.2 Image seeing

The seeing cumulative distributions over the number of tiles is shown Figure 9.

6.3 Tile level spatial astrometric systematics

Figure 10 shows analysis of tile level astrometric systematics from a comparison with stacked residuals from 2MASS stars. There is a systematic effect due to an internal ZPN→TAN definition WCS bug that was fixed for tiles with date of observation after 20120801 which is during ESO observing period 89. All products of observations post-2012801 use the corrected ZPN→TAN transformation. Earlier tile products remain affected at the ∼100mas level by this bug. Pawprint products are unaffected by this WCS bug.

6.4 Other known problems

In the current release, the most common source of spurious images is associated with diffraction halos and filter-reflection ghosts around bright stars; these are localised around the parent star, and are easily

recognised in the parent images. There are also occasional single-band linear features from artificial satellite trails, meteors or aircraft, which can cause a chain of spurious images. Most such spurious images do not match-up between passbands, therefore multi-band matched detections are generally reliable (especially with 2 or more bands), but we emphasise that **all single-band detections should be treated as unreliable,** unless verified by inspection of images.

There are also "bad patches" on certain detectors, namely a large region on Detector#16 (South-East corner) which does not flat-field well, and a strip along an edge of detector#12 which likewise does not correct well and leads to occasional horizontal lines of spurious images.

Cross-talk between detector channels is essentially negligible.

Image persistence (latent images after a bright star lands on a pixel) is generally small, but not quite negligible: since VIRCAM has no shutter, very bright stars can occasionally cause curved "streaks" of persistence as they move in non-straight paths during telescope offsets.

There are a small number (<100) sources in the single band and band-merged catalogs that have very large (>100mag) errors due to them being close to the detection limit. These sources should be flagged manually and will be excluded in future releases. However, given they are so rare ($<0.0006\%$ of the band-merged sources) they should not be a major contaminant in any VHS study.

7   Acknowledgements

Any publication making use of this data, whether obtained from the ESO archive or via third parties, must include the following acknowledgment:

"Based on data products created from observations collected at the European Organisation for Astronomical Research in the Southern Hemisphere under ESO programme 179.A-2010 and made use of data from the VISTA Hemisphere survey (McMahon et al., 2013) with data pipeline processing with the VISTA Data Flow System (Irwin et al., 2004, Lewis et al., 2010, Cross et al., 2012)"

If the access to the ESO Science Archive Facility services was helpful for you research, please include the following acknowledgment:

"This research has made use of the services of the ESO Science Archive Facility. Science data products from the ESO archive may be distributed by third parties, and disseminated via other services, according to the terms of the Creative Commons Attribution 4.0 International license. Credit to the ESO origin of the data must be acknowledged, and the file headers preserved."
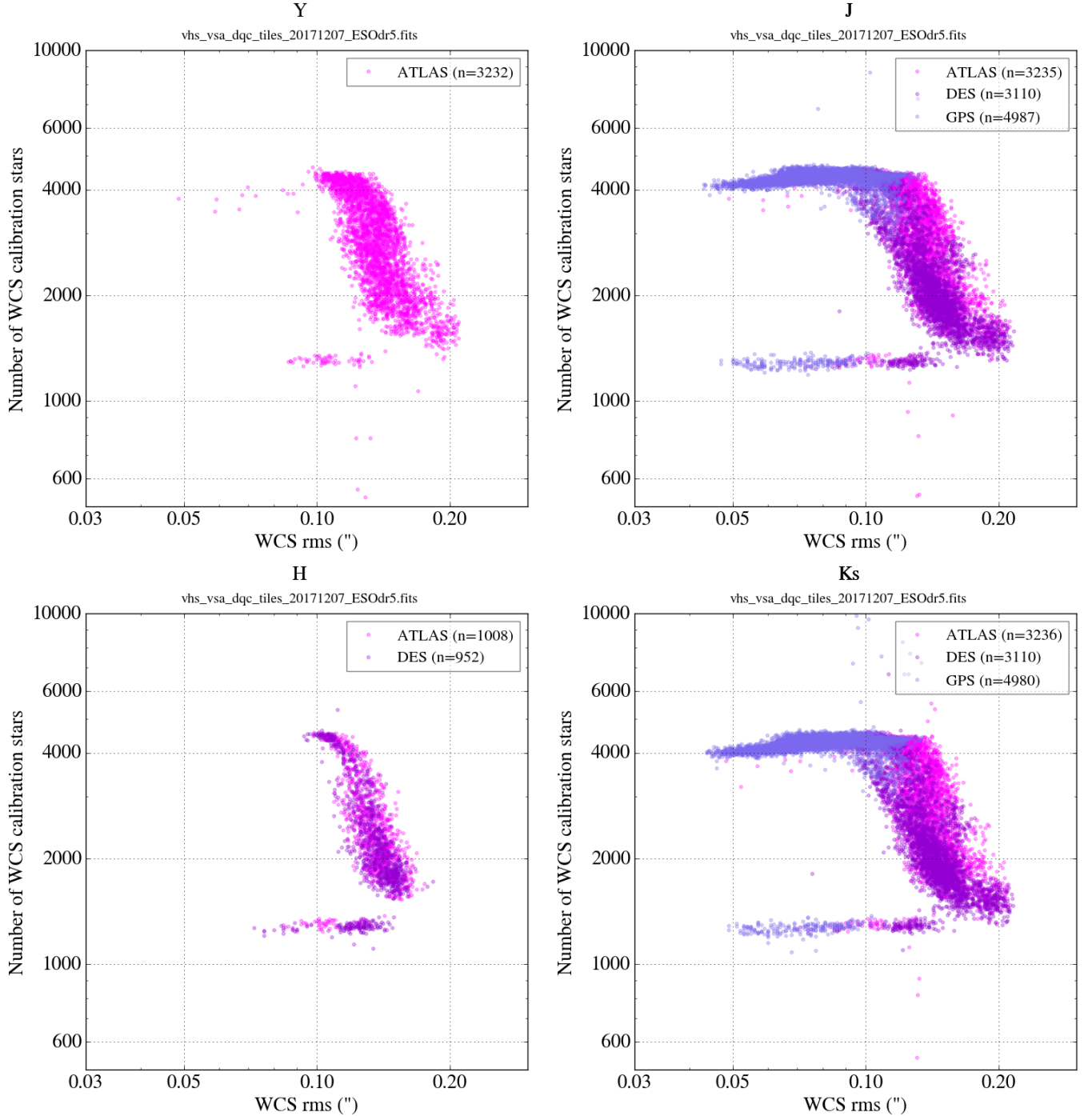
Figure 6: World Cooordinate System (WCS) rms astrometric errors versus number of 2MASS stars used for the WCS fits for tiles. This shows a correlation between the number of stars and the rms residual as expected due to fitting accuracy minimisation. The upper plateau at 4000 stars in the distribution in the J and K_s bands due to upper threshold in number of stars used for the fit which is only reached at low galactic latitude. The horizontal feature at around 1200 stars only appears for data from P84 and P85. The origin of this effect is not currently known and reflect either a real effect in the released data or could be an issue with the casu DQC database. Data is for all tile catalogue observation in DR5.

Version 0.6; March 16, 2020 18:37
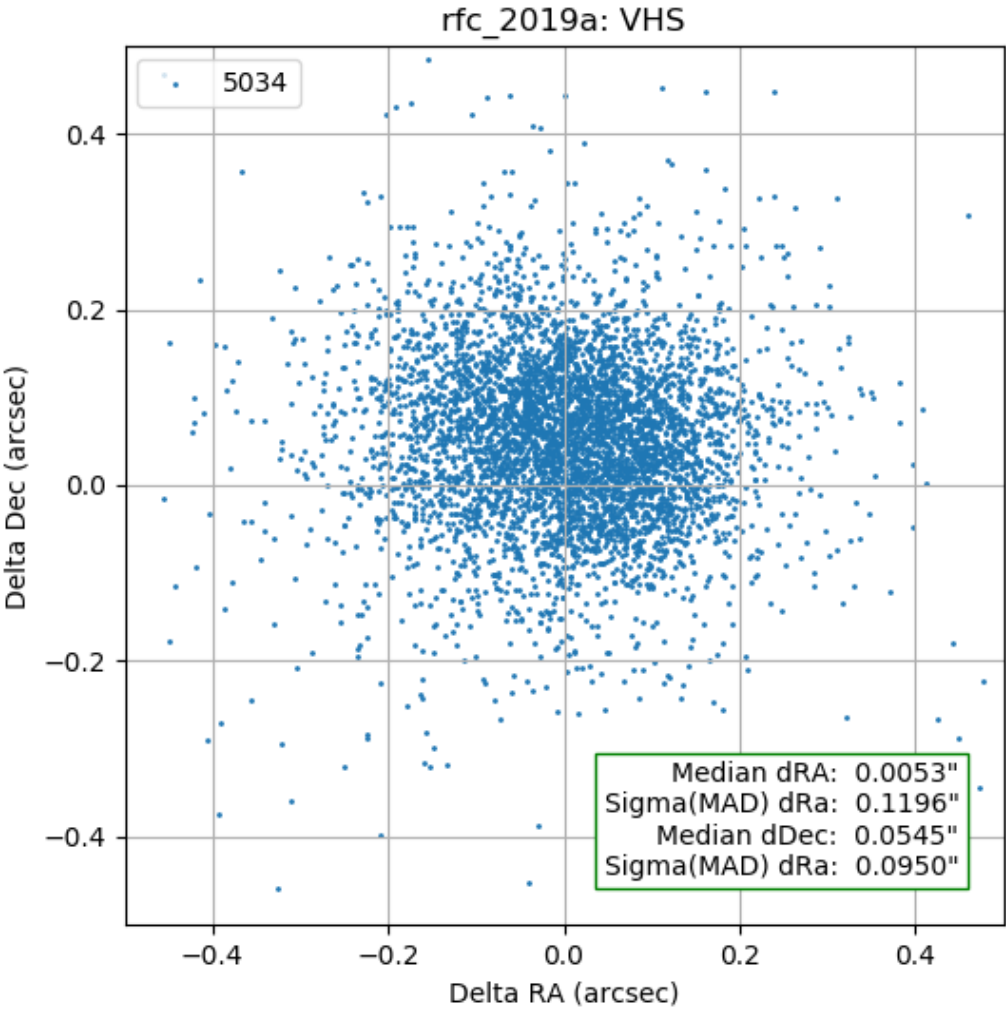
Figure 7: Comparison between VHS DR5 positions and the VLBI radio reference frame
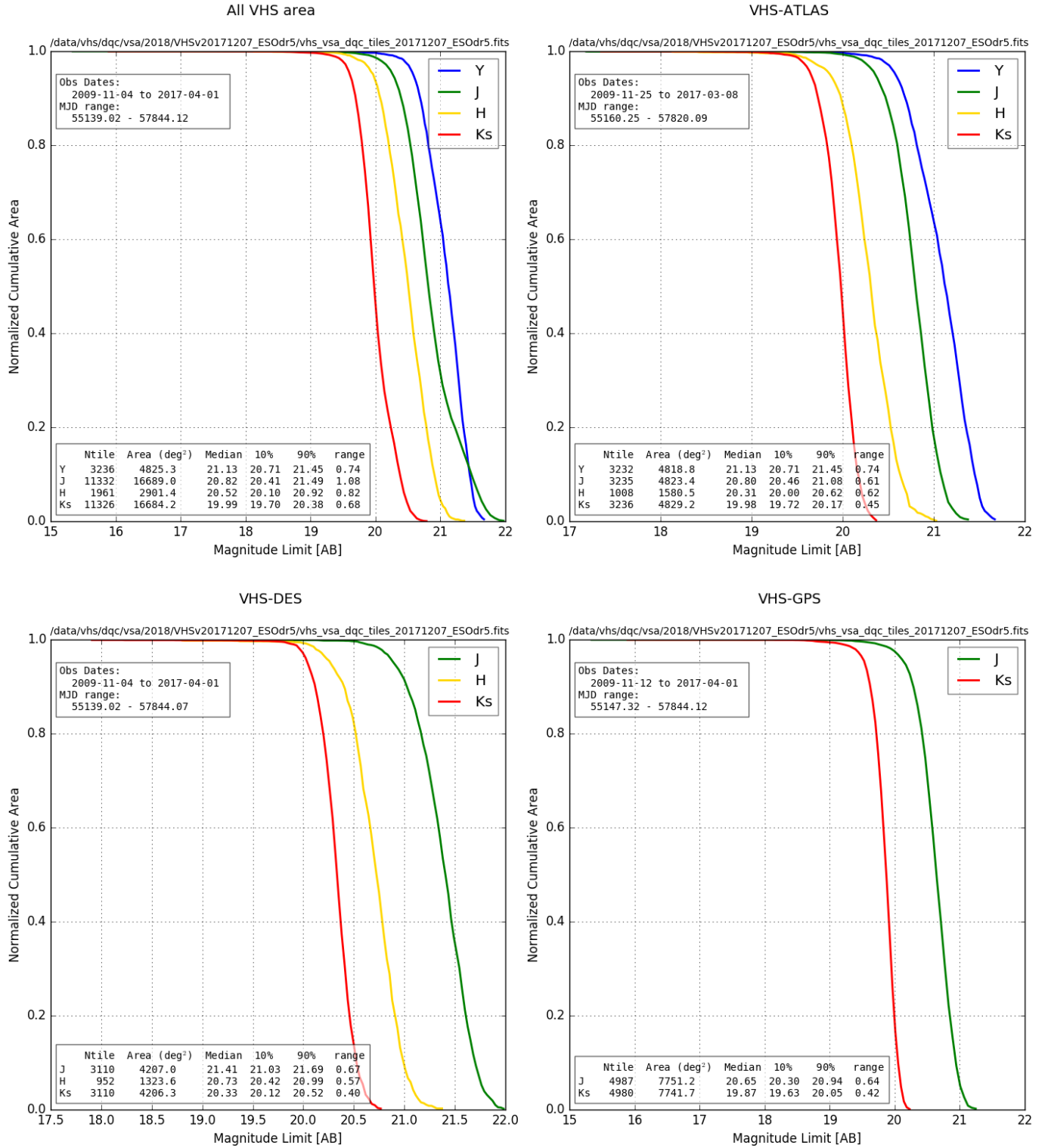
Figure 8: Depth versus cumulative area per band for all observations (top left panel) and for each survey component (ATLAS: top right panel, DES: bottom left panel and GPS: bottom right panel)
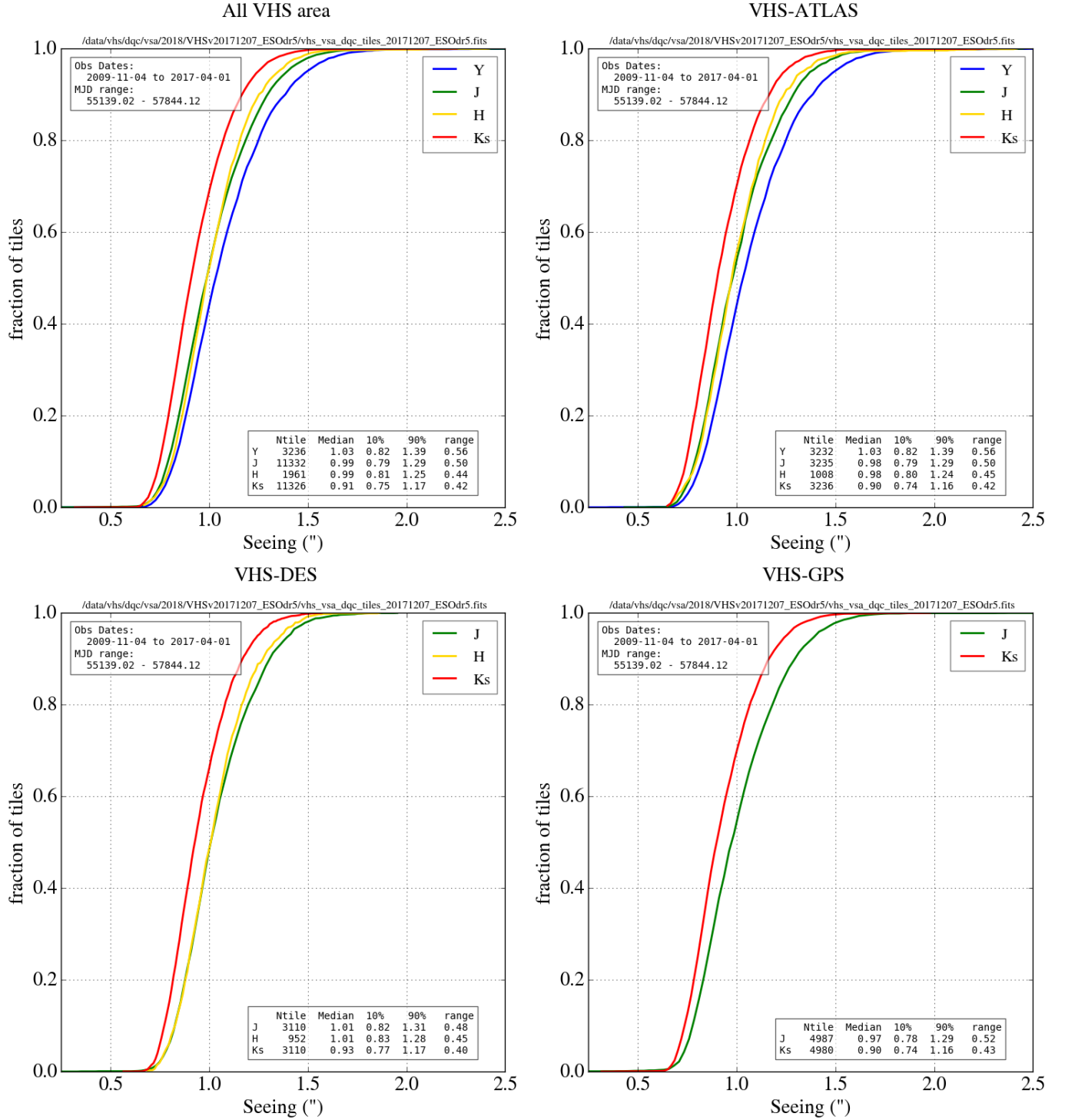
Figure 9: Seeing cumulative distribution over the number of tiles for all observations (top left panel) and for each survey component (ATLAS: top right panel, DES: bottom left panel and GPS: bottom right panel)
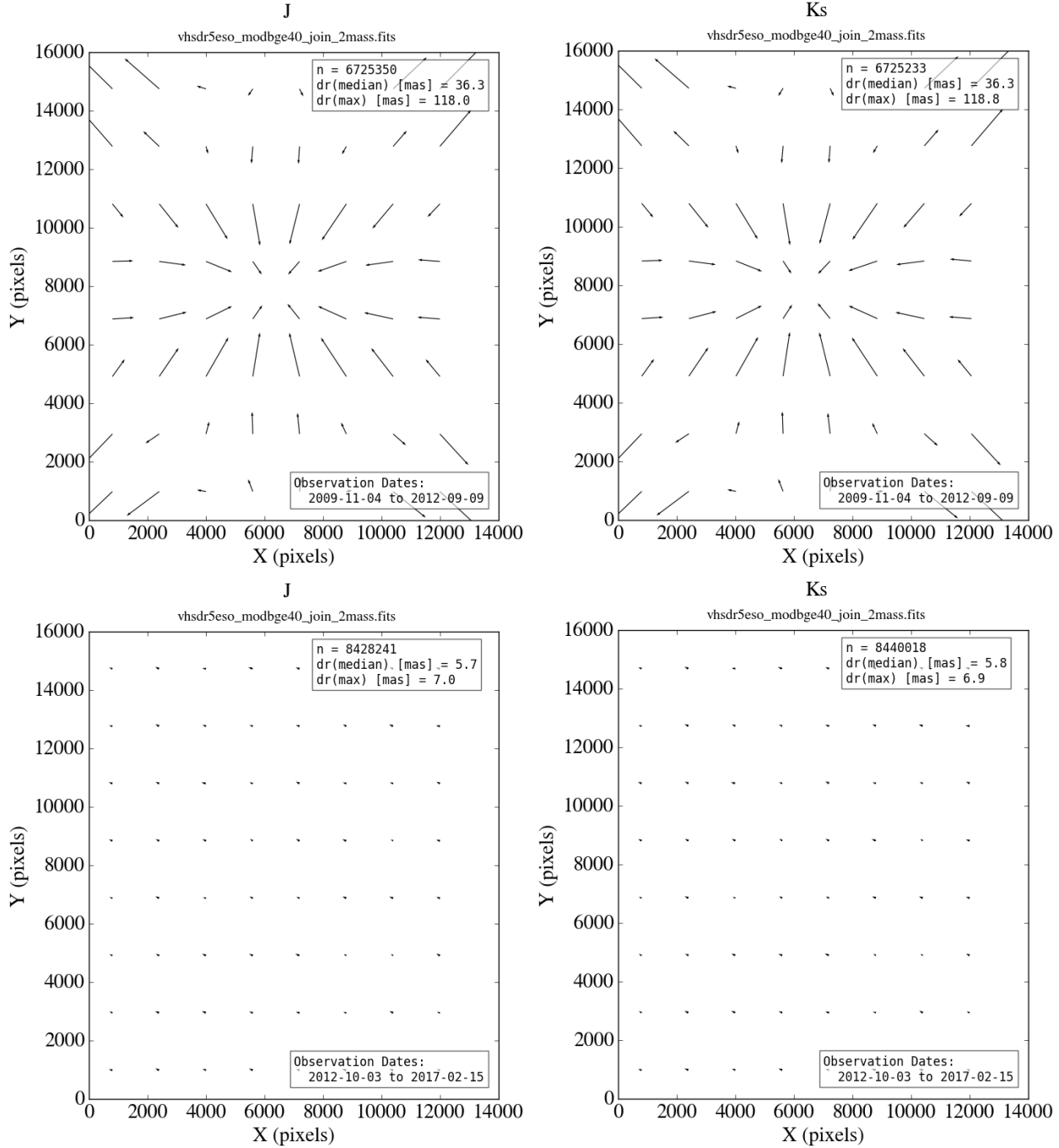
Figure 10: Analysis of Tile level systematics in astrometry from a comparison with stacked residuals from 2MASS stars. This systematic is due to an internal ZPN→TAN definition WCS bug that was fixed for tiles with date of observation after 20120801 which during ESO observing period 89. All products of observations post-20120801 use the corrected ZPN→TAN transformation. Earlier tile products remain affected at the ∼100mas level by this bug. Pawprint products are unaffected by this WCS bug.

Table 4: Tile level multi-band source catalogues column names and description

#	Name	Unit	Description	UCD
1	SOURCENAME		Source name in IAU convention	meta.id
2	SOURCEID		UID of this merged detection as assigned by merge algorithm	meta.id;meta.main
3	CUEVENTID		UID of curation event giving rise to this record	meta.bib
4	FRAMESETID		UID of the set of frames that this merged source comes from	meta.bib
5	RA2000	degrees	Celestial Right Ascension	pos.eq.ra;meta.main
6	DEC2000	degrees	Celestial Declination	pos.eq.dec;meta.main
7	L	degrees	Galactic longitude	pos.galactic.lon
8	B	degrees	Galactic latitude	pos.galactic.lat
9	LAMBDA	degrees	SDSS system spherical co-ordinate 1	pos
10	ETA	degrees	SDSS system spherical co-ordinate 2	pos
11	PRIORSEC		Seam code for a unique (=0) or duplicated (!=0) source	meta.code
12	YMJPNT	mag	Point source colour Y-J (using aperMag3)	phot.color
13	YMJPNTERR	mag	Error on point source colour Y-J	stat.error
14	JMHPNT	mag	Point source colour J-H (using aperMag3)	phot.color
15	JMHPNTERR	mag	Error on point source colour J-H	stat.error
16	HMKSPNT	mag	Point source colour H-K$_s$ (using aperMag3)	phot.color
17	HMKSPNTERR	mag	Error on point source colour H-K$_s$	stat.error
18	JMKSPNT	mag	Point source colour J-K$_s$ (using aperMag3)	phot.color
19	JMKSPNTERR	mag	Error on point source colour J-K$_s$	stat.error
20	YMJEXT	mag	Extended source colour Y-J (using aperMagNoAperCorr3)	phot.color
21	YMJEXTERR	mag	Error on extended source colour Y-J	stat.error
22	JMHEXT	mag	Extended source colour J-H (using aperMagNoAperCorr3)	phot.color
23	JMHEXTERR	mag	Error on extended source colour J-H	stat.error
24	HMKSEXT	mag	Extended source colour H-K$_s$ (using aperMagNoAperCorr3)	phot.color
25	HMKSEXTERR	mag	Error on extended source colour H-K$_s$	stat.error
26	JMKSEXT	mag	Extended source colour J-K$_s$ (using aperMagNoAperCorr3)	phot.color
27	JMKSEXTERR	mag	Error on extended source colour J-K$_s$	stat.error
28	MERGEDCLASSSTAT		Merged N(0,1) stellarness-of-profile statistic	stat
29	MERGEDCLASS		Class flag,1|0|-1|-2|-3|-9=gal|noise|star|probStar|probGal|saturated	meta.code
30	PSTAR		Probability that the source is a star	stat
31	PGALAXY		Probability that the source is a galaxy	stat
32	PNOISE		Probability that the source is noise	stat
33	PSATURATED		Probability that the source is saturated	stat
34	EBV	mag	The galactic dust extinction value measured from the Schlegel maps	phys.absorption.gal
35	AY	mag	The galactic extinction correction in the Y band	phys.absorption.gal
36	AJ	mag	The galactic extinction correction in the J band	phys.absorption.gal
37	AH	mag	The galactic extinction correction in the H band	phys.absorption.gal
38	AKS	mag	The galactic extinction correction in the K$_s$ band	phys.absorption.gal
39	YMJD	days	Modified Julian Day in the Y band	time.epoch
40	YPETROMAG	mag	Extended source Y mag (Petrosian)	phot.mag;em.IR.NIR

#	Name	Units	Description	UCD
41	YPETROMAGERR	mag	Error in extended source Y mag (Petrosian)	stat.error
42	YPSFMAG	mag	Point source profile-fitted Y mag	phot.mag;em.IR.NIR
43	YPSFMAGERR	mag	Error in point source profile-fitted Y mag	stat.error
44	YSERMAG2D	mag	Extended source Y mag (profile-fitted)	phot.mag;em.IR.NIR
45	YSERMAG2DERR	mag	Error in extended source Y mag (profile-fitted)	stat.error
46	YAPERMAG3	mag	Default point source Y aperture corrected mag (2.0 arcsec diam)	phot.mag;em.IR.NIR
47	YAPERMAG3ERR	mag	Error in default point/extended source Y mag	stat.error
48	YAPERMAG4	mag	Point source Y aperture corrected mag (2.8 arcsec aperture diam)	phot.mag;em.IR.NIR
49	YAPERMAG4ERR	mag	Error in point/extended source Y mag (2.8 arcsec aperture diam)	stat.error
50	YAPERMAG6	mag	Point source Y aperture corrected mag (5.7 arcsec aperture diam)	phot.mag;em.IR.NIR
51	YAPERMAG6ERR	mag	Error in point/extended source Y mag (5.7 arcsec aperture diam)	stat.error
52	YAPERMAGNOAPERCORR3	mag	Default extended source Y aperture mag (2.0 arcsec diam)	phot.mag;em.IR.NIR
53	YAPERMAGNOAPERCORR4	mag	Extended source Y aperture mag (2.8 arcsec aperture diameter)	phot.mag;em.IR.NIR
54	YAPERMAGNOAPERCORR6	mag	Extended source Y aperture mag (5.7 arcsec aperture diameter)	em.IR.NIR
55	YHLCORSMJRADAS	arcsecs	Seeing corrected half-light, semi-major axis in Y band	phys.angSize
56	YGAUSIG	pixels	RMS of axes of ellipse fit in Y	src.morph.param
57	YELL		1-b/a, where a/b=semi-major/minor axes in Y	src.ellipticity
58	YPA	degrees	ellipse fit celestial orientation in Y	pos.posAng
59	YERRBITS		processing warning/error bitwise flags in Y	meta.code
60	YAVERAGECONF		average confidence in 2 arcsec diam default aperture 3 Y	stat.likelihood;em.IR.NIR
61	YCLASS		discrete image classification flag in Y	src.class
62	YCLASSSTAT		N(0,1) stellarness-of-profile statistic in Y	stat
63	YPPERRBITS		additional WFAU post-processing error bits in Y	meta.code
64	YSEQNUM		the running number of the Y detection	meta.number
65	YXI	arcsec	Offset of Y detection from master position (+east/-west)	pos.eq.ra;arith.diff
66	YETA	arcsec	Offset of Y detection from master position (+north/-south)	pos.eq.dec;arith.diff
67	JMJD	days	Modified Julian Day in the J band	time.epoch
68	JPETROMAG	mag	Extended source J mag (Petrosian)	em.IR.J
69	JPETROMAGERR	mag	Error in extended source J mag (Petrosian)	stat.error
70	JPSFMAG	mag	Point source profile-fitted J mag	em.IR.J
71	JPSFMAGERR	mag	Error in point source profile-fitted J mag	stat.error
72	JSERMAG2D	mag	Extended source J mag (profile-fitted)	em.IR.J
73	JSERMAG2DERR	mag	Error in extended source J mag (profile-fitted)	stat.error
74	JAPERMAG3	mag	Default point source J aperture corrected mag (2.0 arcsec diam)	em.IR.J
75	JAPERMAG3ERR	mag	Error in default point/extended source J mag	stat.error
76	JAPERMAG4	mag	Point source J aperture corrected mag (2.8 arcsec aperture diam)	em.IR.J
77	JAPERMAG4ERR	mag	Error in point/extended source J mag (2.8 arcsec aperture diam)	stat.error
78	JAPERMAG6	mag	Point source J aperture corrected mag (5.7 arcsec aperture diam)	em.IR.J
79	JAPERMAG6ERR	mag	Error in point/extended source J mag (5.7 arcsec aperture diam)	stat.error
80	JAPERMAGNOAPERCORR3	mag	Default extended source J aperture mag (2.0 arcsec diam)	em.IR.J
81	JAPERMAGNOAPERCORR4	mag	Extended source J aperture mag (2.8 arcsec aperture diameter)	em.IR.J
82	JAPERMAGNOAPERCORR6	mag	Extended source J aperture mag (5.7 arcsec aperture diameter)	em.IR.J
83	JHLCORSMJRADAS	arcsecs	Seeing corrected half-light, semi-major axis in J band	phys.angSize

#	Name	Unit	Description	UCD
84	JGAUSIG	pixels	RMS of axes of ellipse fit in J	src.morph.param
85	JELL		1-b/a, where a/b=semi-major/minor axes in J	src.ellipticity
86	JPA	degrees	ellipse fit celestial orientation in J	pos.posAng
87	JERRBITS		processing warning/error bitwise flags in J	meta.code
88	JAVERAGECONF		average confidence in 2 arcsec diam default aperture 3 J	stat.likelihood;em.IR.NIR
89	JCLASS		discrete image classification flag in J	src.class
90	JCLASSSTAT		N(0,1) stellarness-of-profile statistic in J	stat
91	JPPERRBITS		additional WFAU post-processing error bits in J	meta.code
92	JSEQNUM		the running number of the J detection	meta.number
93	JXI	arcsec	Offset of J detection from master position (+east/-west)	pos.eq.ra;arith.diff
94	JETA	arcsec	Offset of J detection from master position (+north/-south)	pos.eq.dec;arith.diff
95	HMJD	days	Modified Julian Day in the H band	time.epoch
96	HPETROMAG	mag	Extended source H mag (Petrosian)	em.IR.H
97	HPETROMAGERR	mag	Error in extended source H mag (Petrosian)	stat.error
98	HPSFMAG	mag	Point source profile-fitted H mag	em.IR.H
99	HPSFMAGERR	mag	Error in point source profile-fitted H mag	stat.error
100	HSERMAG2D	mag	Extended source H mag (profile-fitted)	em.IR.H
101	HSERMAG2DERR	mag	Error in extended source H mag (profile-fitted)	stat.error
102	HAPERMAG3	mag	Default point source H aperture corrected mag (2.0 arcsec diam)	em.IR.H
103	HAPERMAG3ERR	mag	Error in default point/extended source H mag	stat.error
104	HAPERMAG4	mag	Point source H aperture corrected mag (2.8 arcsec aperture diam)	em.IR.H
105	HAPERMAG4ERR	mag	Error in point/extended source H mag (2.8 arcsec aperture diam)	stat.error
106	HAPERMAG6	mag	Point source H aperture corrected mag (5.7 arcsec aperture diam)	em.IR.H
107	HAPERMAG6ERR	mag	Error in point/extended source H mag (5.7 arcsec aperture diam)	stat.error
108	HAPERMAGNOAPERCORR3	mag	Default extended source H aperture mag (2.0 arcsec diam)	em.IR.H
109	HAPERMAGNOAPERCORR4	mag	Extended source H aperture mag (2.8 arcsec aperture diameter)	em.IR.H
110	HAPERMAGNOAPERCORR6	mag	Extended source H aperture mag (5.7 arcsec aperture diameter)	em.IR.H
111	HHLCORSMJRADAS	arcsecs	Seeing corrected half-light, semi-major axis in H band	phys.angSize
112	HGAUSIG	pixels	RMS of axes of ellipse fit in H	src.morph.param
113	HELL		1-b/a, where a/b=semi-major/minor axes in H	src.ellipticity
114	HPA	degrees	ellipse fit celestial orientation in H	pos.posAng
115	HERRBITS		processing warning/error bitwise flags in H	meta.code
116	HAVERAGECONF		average confidence in 2 arcsec diam default aperture 3 H	stat.likelihood;em.IR.NIR
117	HCLASS		discrete image classification flag in H	src.class
118	HCLASSSTAT		N(0,1) stellarness-of-profile statistic in H	stat
119	HPPERRBITS		additional WFAU post-processing error bits in H	meta.code
120	HSEQNUM		the running number of the H detection	meta.number
121	HXI	arcsec	Offset of H detection from master position (+east/-west)	pos.eq.ra;arith.diff
122	HETA	arcsec	Offset of H detection from master position (+north/-south)	pos.eq.dec;arith.diff
123	KSMJD	days	Modified Julian Day in the K_s band	time.epoch
124	KSPETROMAG	mag	Extended source K_s mag (Petrosian)	em.IR.K
125	KSPETROMAGERR	mag	Error in extended source K_s mag (Petrosian)	stat.error
126	KSPSFMAG	mag	Point source profile-fitted K_s mag	em.IR.K

#	Name	Units	Description	UCD
127	KSPSFMAGERR	mag	Error in point source profile-fitted K_s mag	stat.error
128	KSSERMAG2D	mag	Extended source K_s mag (profile-fitted)	em.IR.K
129	KSSERMAG2DERR	mag	Error in extended source K_s mag (profile-fitted)	stat.error
130	KSAPERMAG3	mag	Default point source K_s aperture corrected mag (2.0 arcsec diam)	em.IR.K
131	KSAPERMAG3ERR	mag	Error in default point/extended source K_s mag	stat.error
132	KSAPERMAG4	mag	Point source K_s aperture corrected mag (2.8 arcsec aperture diam)	em.IR.K
133	KSAPERMAG4ERR	mag	Error in point/extended source K_s mag (2.8 arcsec aperture diam)	stat.error
134	KSAPERMAG6	mag	Point source K_s aperture corrected mag (5.7 arcsec aperture diam)	em.IR.K
135	KSAPERMAG6ERR	mag	Error in point/extended source K_s mag (5.7 arcsec aperture diam)	stat.error
136	KSAPERMAGNOAPERCORR3	mag	Default extended source K_s aperture mag (2.0 arcsec diam)	em.IR.K
137	KSAPERMAGNOAPERCORR4	mag	Extended source K_s aperture mag (2.8 arcsec aperture diameter)	em.IR.K
138	KSAPERMAGNOAPERCORR6	mag	Extended source K_s aperture mag (5.7 arcsec aperture diameter)	em.IR.K
139	KSHLCORSMJRADAS	arcsecs	Seeing corrected half-light, semi-major axis in K_s band	phys.angSize
140	KSGAUSIG	pixels	RMS of axes of ellipse fit in K_s	src.morph.param
141	KSELL		1-b/a, where a/b=semi-major/minor axes in K_s	src.ellipticity
142	KSPA	degrees	ellipse fit celestial orientation in K_s	pos.posAng
143	KSERRBITS		processing warning/error bitwise flags in K_s	meta.code
144	KSAVERAGECONF		average confidence in 2 arcsec diam default aperture 3 K_s	stat.likelihood;em.IR.NIR
145	KSCLASS		discrete image classification flag in K_s	src.class
146	KSCLASSSTAT		N(0,1) stellarness-of-profile statistic in K_s	stat
147	KSPPERRBITS		additional WFAU post-processing error bits in K_s	meta.code
148	KSSEQNUM		the running number of the K_s detection	meta.number
149	KSXI	arcsec	Offset of K_s detection from master position (+east/-west)	pos.eq.ra;arith.diff
150	KSETA	arcsec	Offset of K_s detection from master position (+north/-south)	pos.eq.dec;arith.diff
151	PRIMARY_SOURCE		Flag indicates primary sources (=1), otherwise (=0)	meta.code

References

Cross N. J. G., et al., 2012, A&A, 548, A119

Dalton G. B., et al., 2006, The VISTA infrared camera. Proc. SPIE, p. 62690X, doi:10.1117/12.670018

González-Fernández C., et al., 2018, MNRAS, 474, 5459

Hamilton A. J. S., Tegmark M., 2004, MNRAS, 349, 115

Irwin M. J., et al., 2004, VISTA data flow system: pipeline processing for WFCAM and VISTA. Proc. SPIE, pp 411–422, doi:10.1117/12.551449

Lewis J. R., Irwin M., Bunclark P., 2010, Pipeline Processing for VISTA. ASP Conf. Ser., p. 91

McMahon R. G., Banerji M., Gonzalez E., Koposov S. E., Bejar V. J., Lodieu N., Rebolo R., VHS Collaboration 2013, The Messenger, 154, 35

Skrutskie M. F., et al., 2006, , 131, 1163

Sutherland W., et al., 2015, A&A, 575, A25

Swanson M. E. C., Tegmark M., Hamilton A. J. S., Hill J. C., 2008, MNRAS, 387, 1391